ISSN 0021-3640, JETP Letters, 2009, Vol. 89, No. 12, pp. 632–637. © Pleiades Publishing, Ltd., 2009.
Original Russian Text © I.A. Makarov, S.G. Ovchinnikov, E.I. Shneider, 2009, published in Pis'ma v Zhurnal Éksperimental'noĭ i Teoreticheskoĭ Fiziki, 2009, Vol. 89, No. 12, pp. 736–741.

Reconstruction of the Fermi Surface of HTSC Cuprates in a High Magnetic Field

I. A. Makarov[a, *], S. G. Ovchinnikov[a, b], and E. I. Shneider[a, c]

[a] *Kirensky Institute of Physics, Siberian Branch, Russian Academy of Sciences, Krasnoyarsk, 660036 Russia*
**e-mail: macplay@mail.ru*
[b] *Siberian Federal University, Krasnoyarsk, 660041 Russia*
[c] *Reshetnev Siberian State Aerospace University, Krasnoyarsk, 660014 Russia*

Received May 18, 2009

The effect of a high magnetic field on the electronic structure of HTSC cuprates is considered. The study is performed in the t–t'–t''–J^* model, and the high magnetic field effect is taken into account not only as the Zeeman splitting of the one-electron levels, but also in the occupation numbers of the states with different spin projections and in the formation of the spin correlation functions. The field is assumed to be high enough to align all of the spins along the field. As a result, the Fermi surface reconstruction is obtained from four hole pockets about the nodal point $(\pi/2, \pi/2)$ in the paramagnetic phase to a large hole pocket about the point (π, π) in the ferromagnetic phase. As the magnetic field strength decreases, a number of quantum phase transitions are revealed; they are manifested in the changed Fermi surface topology. The Fermi surface reconstruction with a decreasing field is qualitatively the same as that with an increasing doping degree in the absence of a magnetic field.

PACS numbers: 71.18.+y, 73.43.Nq, 74.25.Jb, 74.72.-h
DOI: 10.1134/S002136400912008X

1. Although the electronic structure of the HTSC cuprates is their most important characteristic in the normal phase, it does not yet have any commonly accepted representation. The authors of various theoretical and experimental studies suggest their own patterns of the band structure and Fermi surface. In particular, in the ARPES experiments [1] on weakly doped LSCO, the Fermi surface consists of four arcs, while in [2] studying the $Na_{2-x}Ca_xCu_2O_2Cl_2$ compound, these arcs are so stretched that they can be considered as hole pockets. The latter statement is supported by the studies of quantum oscillations [3] where the area of the two-dimensional Fermi surface and, hence, the number of carriers in the system were measured. Since the number of holes suggested in those experiments did not correspond to the actual doping degree of the compound, the authors concluded that there are electron portions of the Fermi surface that are ARPES-invisible. The same conclusion was made in the studies of the Hall effect on single and double-layer cuprates [4] where the Hall constant changed its sign as the temperature decreased, thus indicating a change of the major carrier type. However, in connection to those papers, we attract attention to the different experimental conditions, rather than to different electronic structure patterns. Since the ARPES experiments are performed in the absence of a magnetic field, while the quantum oscillations and the Hall effect are observed only in a high magnetic field, the questions naturally arise: is it possible to compare these results, and, generally, how does a magnetic field affect the electronic structure? In this work, we have studied this effect and revealed the variation of the Fermi surface topology in a high magnetic field on the example of the single-layer $La_{2-x}Sr_xCuO_4$ cuprate. In the investigations, the t–t'–t''–J^* model is used whose parameters are derived from the microscopic multiband p–d model. Along with the Zeeman splitting of energy-degenerate single-particle states with different spin projections, the field also affects the occupation numbers of the corresponding states and the spin correlation functions, and the latter effect will prevail. The magnetic field is assumed to be high enough to align the spins in the sites in one direction (we assume the spin up), while the flip to the state with the opposite spin projection is possible due to the finite temperature. It is shown that the Fermi surface in the paramagnetic–ferromagnetic phase transition changes the orientation centered about the point $(\pi/2, \pi/2)$ to that centered about the point (π, π) for the spin-down (opposite to the field direction) quasiparticle band. As the magnetic field magnitude varies, a series of quantum phase transitions manifested in a variation of the Fermi surface topology for the spin-up quasiparticle band occur in the ferromagnetic phase itself.

2. In our investigation of the HTSC cuprates, we start from the single-layer $La_{2-x}Sr_xCuO_4$ compound.

Since this compound is a system with strong electronic correlations, we reduce the initial many-band p–d Hubbard model with the real parameters obtained in the LDA–GTB scheme [5] (the LDA ab initio calculations + the generalized tight-binding scheme [6]) in the low-energy excitation region to the t–J^* model obtained from the Hubbard model in the limit $U \gg t$ [7–10]. This model is written for hole excitations, which form the quasiparticle bands described by the Hubbard operators $X_f^{\sigma S} = |\sigma\rangle\langle S|$ and $X_f^{\bar{\sigma} S} = |\bar{\sigma}\rangle\langle S|$, where $|\sigma\rangle$ is the local state of one hole with the spin projection σ, and $|S\rangle$ is the two-hole Zhang–Rice singlet. The microscopic theory [5] implies the necessity of the inclusion of hops to the other cells to the third-nearest neighbor inclusively. Therefore, the t–J^* model is reduced to the t–t'–t''–J^* model (J^* means that not only the exchange terms, but also the three-center correlated hops are taken into account). In the magnetic field, a doubly degenerate single-particle state in the paramagnetic phase is split into the states with energies $\epsilon_1 - \mu_B H$ and $\epsilon_1 + \mu_B H$. The correction $\mu_B H$ attributed to the interaction between spin and magnetic field is small (about 0.01 eV) even at the field strength of 300 T. The occupation numbers of the single-particle states can be determined by jointly solving the equations for the chemical potential

$$1 + x = \sum_{\sigma} p_{\sigma} + 2\langle X^{SS}\rangle, \tag{1}$$

where x is the hole doping degree and the basis completeness conditions are

$$\sum_{\sigma} X^{\sigma\sigma} + X^{SS} = 1. \tag{2}$$

The total number of states for the one-particle sector of the Gilbert space is $\sum_{\sigma} p_{\sigma} = 1 - x$. The occupation number for the state with the spin projection σ directed along the field is

$$p_{\sigma} = \langle X_f^{\sigma\sigma}\rangle = (1 - n_0)(1 - x) \tag{3}$$

and

$$p_{\bar{\sigma}} = \langle X_f^{\bar{\sigma}\bar{\sigma}}\rangle = n_0(1 - x) \tag{4}$$

for the spin-down state. Here, n_0 is the concentration of the spins opposite to the field direction at a certain temperature,

$$n_0 = \frac{1}{1 + \exp\left(\dfrac{2\mu_B H}{kT}\right)}. \tag{5}$$

Thus, the Hamiltonian of the t–t'–t''–J^* model is

$$\begin{aligned} H = &\sum_{f\sigma} (\varepsilon_1 - 2\sigma\mu_B H - \mu) X_f^{\sigma\sigma} \\ &+ \sum_{f} (\varepsilon_2 - 2\mu) X_f^{SS} \\ &+ \sum_{fg\sigma} t_{fg} X_f^{S\sigma} X_g^{\sigma S} + \sum_{fg\sigma} J_{fg} (X_f^{\sigma\bar{\sigma}} X_g^{\bar{\sigma}\sigma} - X_f^{\sigma\sigma} X_g^{\bar{\sigma}\bar{\sigma}}) \\ &- \sum_{m\ln\sigma} \frac{\bar{t}_{ml} \tilde{t}_{\ln}}{E_{ct}} (X_m^{S\sigma} X_l^{\sigma\bar{\sigma}} X_n^{\bar{\sigma} S} - X_m^{S\sigma} X_l^{\bar{\sigma}\bar{\sigma}} X_n^{\sigma S}), \end{aligned} \tag{6}$$

where $J_{fg} = 2\tilde{t}_{fg}^2 / E_{ct}$ is the constant of the effective exchange interaction due to the hops to a lower Hubbard band and back, t_k is the intraband intercell hops, $\tilde{t}_k$ is the interband intercell hops, and E_{ct} is the dielectric gap with the charge transfer.

To determine the spectrum of quasiparticle excitations, we use the method of the motion equations to construct the Green's function $\langle\langle X_f^{\alpha} | X_g^{+\beta}\rangle\rangle$ on the Hubbard operators. The reduced Green's function is an element of the matrix Green's function relating to the ordinary two-time retarded Green's function $G(\mathbf{r}, E) = \langle\langle c_{f+r} | c_f^{+}\rangle\rangle_E$ by the expression

$$G(\mathbf{r}, E) = \sum_{\alpha,\beta} \gamma_{\sigma}(\alpha)\gamma_{\sigma}^{*}(\beta) D^{\alpha\beta}(\mathbf{r}, E), \tag{7}$$

where the coefficients $\gamma(\alpha)$ are directly determined from the products of the cell wavefunctions involved in the transition with the root vector α. The exact equation of motion for the operator $X_f^{\sigma S}$ has the form

$$i\dot{X}_f^{\sigma S} = [X_f^{\sigma S}, H] = (\varepsilon_2 - \varepsilon_1 - \mu + 2\mu_B H) X_f^{\sigma S} + L_f^{\sigma S}, \tag{8}$$

where $L_f^{\sigma S}$ includes the terms forming the higher-order Green's functions. To project them onto the single-particle operator basis, we use the method of irreducible operators applied earlier in [11–13]. In accordance with this method, the operator $L_f^{\sigma S}$ is transformed as follows:

$$L_f^{\sigma S} = \sum_{s\beta} T_f^{(\sigma S)\beta} X_s^{\beta} + L_f^{\sigma S(\mathrm{irr})}, \tag{9}$$

where

$$T_f^{(\sigma S)\beta} = \langle\{L_f^{\sigma S}, X_s^{+\beta}\}\rangle / \langle\{X_s^{\beta}, X_s^{+\beta}\}\rangle. \tag{10}$$

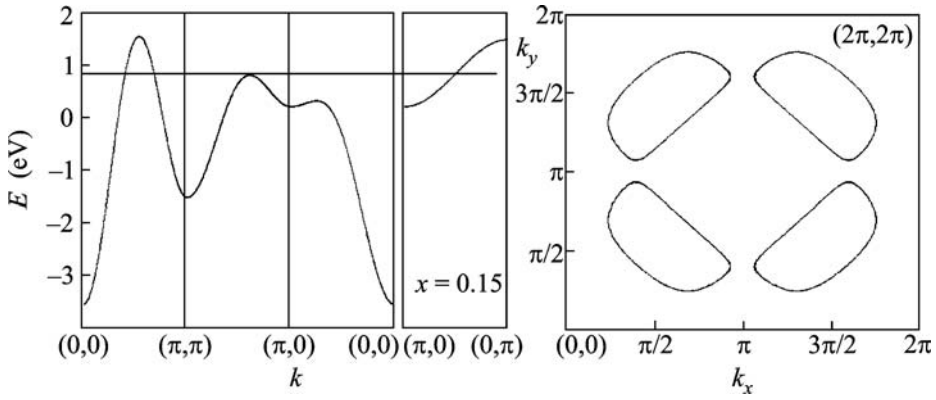

Fig. 1. Band structure and Fermi surface for the paramagnetic phase ($x = 0.15$).

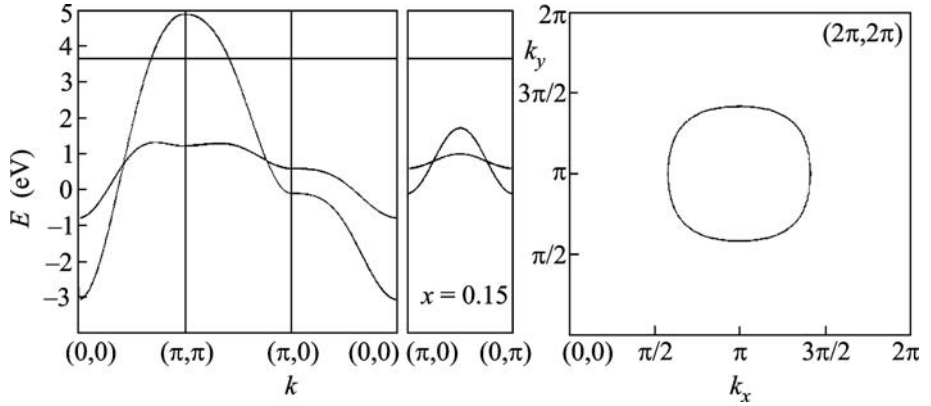

Fig. 2. Band structure and Fermi surface for the ferromagnetic phase ($T = 10$ K, $H = 300$ T, and $x = 0.15$). The wide and narrow bands correspond to the spin-down and spin-up quasiparticles.

The kinetic $\langle X_f^{S\sigma} X_g^{\sigma S}\rangle$ and spin $\langle X_f^{\sigma\bar{\sigma}} X_g^{\bar{\sigma}\sigma}\rangle$ correlation functions separated in the averaging process are important characteristics of the system and considerably affect the electronic structure [11–13]. Since we believe that the field applied to our compound is high enough to order all spins in one direction, we obtain the spin correlation functions of the ferromagnetic type independent of the distance,

$$\langle X_f^{\sigma\bar{\sigma}} X_g^{\bar{\sigma}\sigma}\rangle = 0, \quad \langle X_f^{\sigma\sigma} X_g^{\sigma\sigma}\rangle = p_\sigma^2.$$

The kinetic correlation functions are calculated self-consistently by the spectral theorem with the Green's function

$$\langle\langle X_k^{\sigma S} | X_k^{S\sigma}\rangle\rangle = \frac{p_\sigma + x}{E - E_{k\sigma}}, \tag{11}$$

and

$$E_{k\sigma} = \varepsilon_2 - \varepsilon_1 - \mu + 2\mu_B H + (p_\sigma + x)t_k + p_{\bar{\sigma}} J_0 + p_{\bar{\sigma}}(p_\sigma + x)\frac{\tilde{t}_k^2}{E_{ct}} + \Sigma_\sigma(k); \tag{12}$$

while the mass operator is

$$\Sigma_\sigma(k) = \frac{1}{p_\sigma + xN}\frac{1}{\times \sum_q \left[t_q - J_{k-q} - x\frac{\tilde{t}_q^2}{E_{ct}} - (p_\sigma + x)\frac{2\tilde{t}_q\tilde{t}_k}{E_{ct}}\right] K_q,}$$

where K_q is the Fourier image of the kinetic correlation function.

3. The paramagnetic phase study repeats the results of work [13], where it was shown that the system exhibits short-range antiferromagnetic correlations, which appear when the spin correlation functions are taken into account. These correlations transform the band structure to the form typical of the antiferromagnetic phase with the maximum at the point $(\pi/2, \pi/2)$ (Fig. 1) for weakly doped compounds. The applied field separates the single-particle state with spin σ and, hence, the state corresponding to the quasiparticle excitation with spin $\bar{\sigma}$, which forms a wide band with the maximum at the point (π, π) (Fig. 2). The considerable width of this band (about 8 eV) is due to the

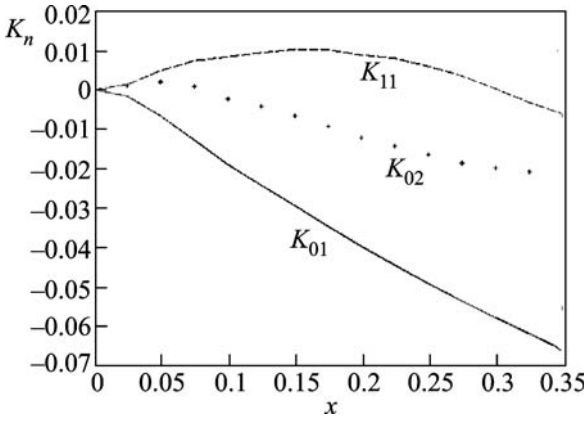

Fig. 3. Critical correlation functions versus the doping degree in the ferromagnetic phase.

term $(p_\sigma + x)t_k$ in relation (12). The other narrow band describes the quasiparticle with spin σ, which characterizes the transition from the lower-probability state $\bar{\sigma}$ to the singlet state. It is seen that the Fermi surface undergoes qualitative changes with applying the field: it is transformed from four hole pockets around (π/2, π/2) into a single large hole pocket around (π, π).

The band structure presented for the ferromagnetic phase was obtained taking into account the self-consistently calculated kinetic correlation functions. Figure 3 shows the doping degree dependence of the kinetic correlation functions. The correlation function between the nearest neighbors has the greatest magnitude K_{01}, which increases almost linearly with the number of hole carriers. The correlations between the second-nearest neighbors K_{11} increase in the positive

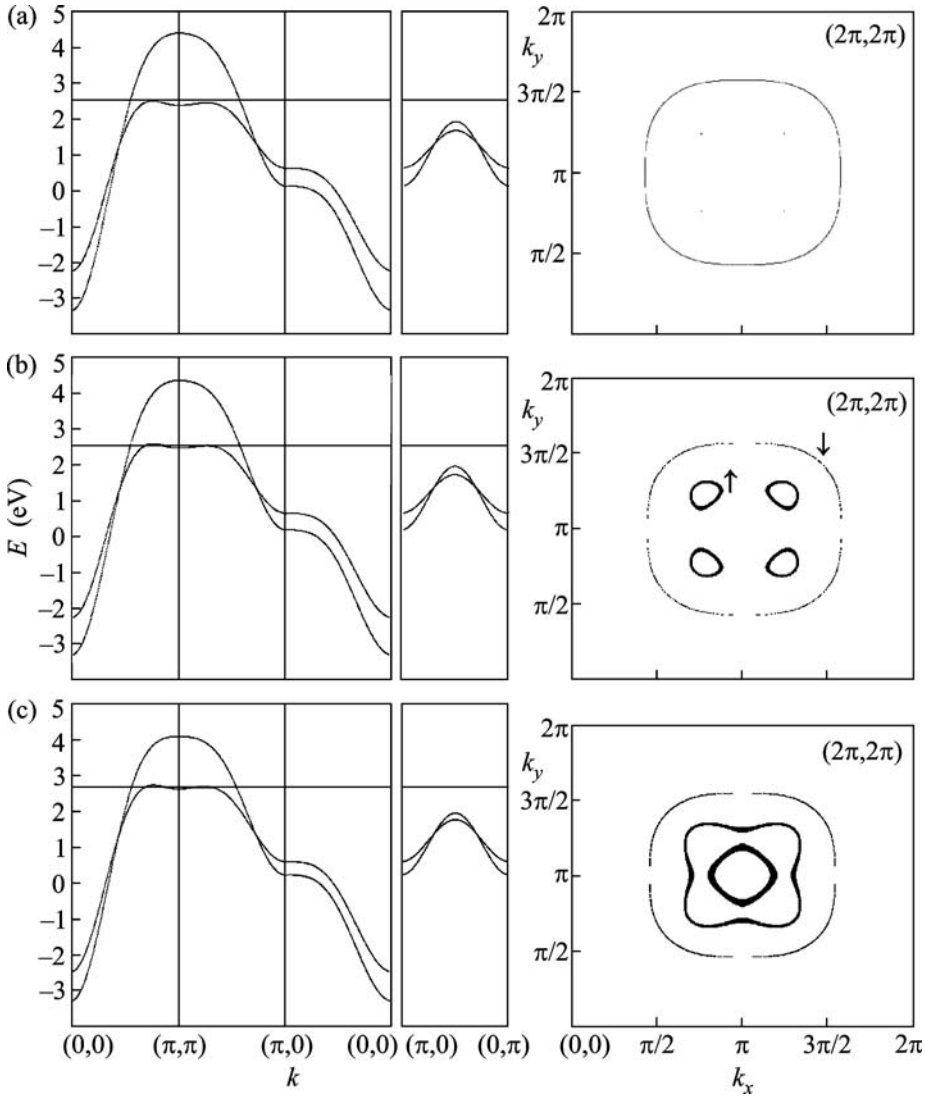

Fig. 4. Band structure and Fermi surface of LSCO for different spin projections at $T = 150$ K; $x = 0.25$; and $H =$ (a) 122, (b) 121, and (c) 117 T.

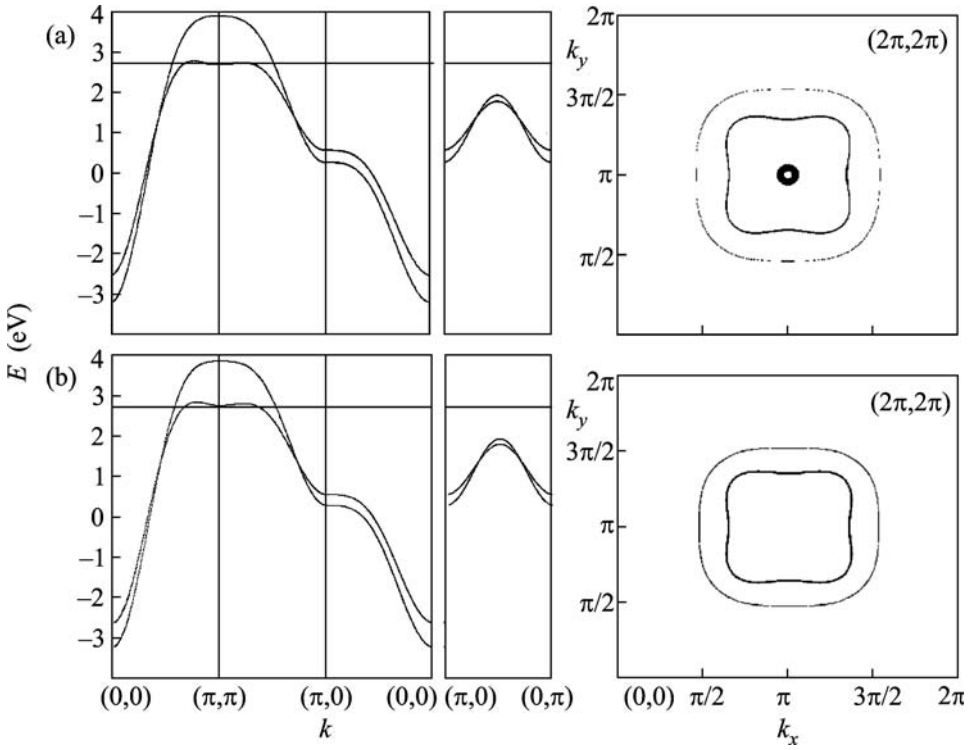

Fig. 5. Band structure and Fermi surface of LSCO for different spin projections at $T = 150$ K, $x = 0.25$, and $H =$ (a) 109 and (b) 105 T.

region up to the optimal doping level, and then they decrease and change sign near $x = 0.3$. The reason why the spin-down band is much wider than the spin-up one is rather trivial. In a high magnetic field, all spins on each cell site at $x = 0$ are directed upward. It is impossible to add a spin-up hole due to the Pauli principle, and only doping generates the Zhang–Rice singlets and allows the up-spin holes to move. Spin fluctuations at a finite temperature play a similar role. Therefore, the kinetic energy of the spin-up holes is proportional to $x + p_{\bar{\sigma}} \ll 1$. Meanwhile, the spin-down hole freely moves against the background of the undoped ferromagnetic dielectric state. The situation is similar to the spin polaron in a ferromagnetic semiconductor [14, 15]. Since the Zhang–Rice singlet is formed when the second hole is added to the site, this corresponds to the problem of a polaron with an antiferromagnetic carrier–spin exchange interaction. We also notice that the band structure shown in Fig. 2 corresponds to the state of a spin semimetal where only the states with a single spin projection are present at the Fermi level [16]. In other words, the 100% spin polarization of the current carriers exists in this state.

4. A number of Lifshitz phase transitions are clearly observed when the field and temperature are of the same order of magnitude [17, 18]. This picture takes place when the temperature is sufficient to increase the narrow band width to the required value due to an increase in the occupancy of the single-particle level with spin $\bar{\sigma}$. Under these conditions, the chemical potential lies in a narrower band and the Fermi surface varies considerably. We investigate the evolution of the Fermi surface at the constant doping level $x = 0.25$ and $T = 150$ K by varying the field strength H. Up to $H =$ 122 T, the situation is qualitatively the same as that in Fig. 2: a large spin-down hole pocket exists. In magnetic fields higher than $H = 122$ T, four additional spin-up pockets start to develop in addition to the initial hole pocket (see Fig. 4a). This corresponds to the ratio $H/T \approx 0.8$. As the field decreases further, the hole pockets grow larger (Fig. 4b), and then they form a single electron pocket and a single hole region of an intricate shape (Fig. 4c). The subsequent evolution is presented in Fig. 5. The electron pocket decreases gradually (see Fig. 5a) and disappears at $H/T = 0.7$ leaving two large hole pockets on the Fermi surface (see Fig. 5b). Therefore, depending on the field magnitude, different relations of the hole and electron carriers are feasible in the system.

5. In this work, we have considered the effect of a magnetic field on the band structure and the Fermi surface in the simplest approximation (with respect to magnetic correlations). It has appeared that the band structure and the Fermi surface for $La_{2-x}Sr_xCuO_4$ in a high field differ considerably from the situation in the paramagnetic phase, and this is caused by the suppression of antiferromagnetic correlation. As the magnetic field decreases at temperatures energy-comparable

with the field energy, some transformations of the Fermi surface are observed, which are the quantum phase transitions [17, 18]. The picture of the transformations is very similar to that in the paramagnetic phase as the doping degree increases [11–13]. The changes occur because the spin-up quasiparticle band is wide enough to cross the chemical potential. We note that it is unlikely that the antiferromagnetic correlations are completely suppressed for the real fields of 50–60 T at which the quantum oscillations have been measured to date. According to the measurements on the La_2CuO_4 single crystals [19], the spin-orientation transition occurs at $H \approx 5$ T, so that the ferromagnetic component at $H > 5$ T already exists. Nonetheless, the fields $H \sim 50$ T are intermediate so that the ferromagnetic and antiferromagnetic components of spin correlations are simultaneously present. Therefore, the study of the electronic structure in these fields requires an additional calculation of the spin correlation functions in the external field. This will be the subject of our next work.

This work was supported by the Russian Foundation for Basic Research (project no. 09-02-00127), the Siberian Branch and the Ural Division, Russian Academy of Sciences (integration project no. 40), and the Presidium of the Russian Academy of Sciences (program no. 5.7).

REFERENCES

1. T. Yoshida, X. J. Shou, et al., Phys. Rev. B **74**, 224510 (2006).
2. K. Shen et al., Science **307**, 901–904 (2005).
3. N. Doiron-Leyraud et al., Nature **447**, 565 (2007).
4. D. LeBoeuf, N. Doiron-Leyraud, et al., Nature **450**, 533 (2007).
5. M. Korshunov, V. Gavrichkov, S. Ovchinnikov, et al., Phys. Rev. B **72**, 165104 (2005).
6. S. G. Ovchinnikov and I. S. Sandalov, Physica C **161**, 607 (1989).
7. L. N. Bulaevskii, E. L. Nagaev, and D. I. Khomskii, Zh. Eksp. Teor. Fiz. **54**, 1562 (1968) [Sov. Phys. JETP **27**, 836 (1968)].
8. K. A. Chao, J. Spalek, and A. M. Oles, J. Phys. C **10**, L271 (1977).
9. J. E. Hirsch, Phys. Rev. Lett. **54**, 1317 (1985).
10. V. I. Belinicher, A. L. Chernyshev, and V. A. Shubin, Phys. Rev. B **53**, 335 (1996).
11. N. M. Plakida and V. S. Oudovenko, Phys. Rev. B **59**, 11949 (1999).
12. V. V. Val'kov and D. M. Dzebisashvili, Zh. Eksp. Teor. Fiz. **127**, 686 (2005) [JETP **100**, 608 (2005)].
13. M. Korshunov and S. Ovchinnikov, Eur. Phys. J. B **57**, 271 (2007).
14. E. L. Nagaev, Zh. Eksp. Teor. Fiz. **56**, 1013 (1969) [Sov. Phys. JETP **29**, 545 (1969)].
15. Yu. A. Izyumov and M. V. Medvedev, Zh. Eksp. Teor. Fiz. **59**, 553 (1970) [Sov. Phys. JETP **32**, 302 (1970)].
16. V. Yu. Irkhin and M. I. Katsnel'son, Usp. Fiz. Nauk **164**, 705 (1994) [Phys. Usp. **37**, 659 (1994)].
17. I. M. Lifshitz, Zh. Eksp. Teor. Fiz. **38**, 1569 (1960) [Sov. Phys. JETP **11**, 1130 (1960)].
18. I. M. Lifshitz, M. Ya. Azbel, and M. I. Kaganov, *Electron Theory of Metals* (Nauka, Moscow, 1971; Consultants Bureau, New York, 1973).
19. A. D. Balaev, A. B. Bykov, L. N. Dem'yanets, et al., Zh. Eksp. Teor. Fiz. **100**, 1365 (1991) [Sov. Phys. JETP **73**, 756 (1991)].

Translated by E. Perova